UNIVERSITÉ BOURGOGNE FRANCHE-COMTÉ

MASTERS THESIS

Is it possible to characterize neuronal activity using magnetic resonance?

Author:
Neha Binish

Supervisor:
David VIENNOT

A thesis submitted in fulfillment of the requirements for the degree of Master Computational Physics

in the

Department of Physics

June 24, 2021

UNIVERSITÉ BOURGOGNE FRANCHE-COMTÉ

Abstract

Department of Physics

Master Computational Physics

Is it possible to characterize neuronal activity using magnetic resonance?

by Neha Binish

The brain is an inherently complex organ with intricate structure and behaviour. A part of this complexity is accounted to its ability to function at several different scales, both in the temporal and spatial domains. Currently, we have two non-invasive techniques; MRI and EEG, to map the neuronal activity in the brain. The inexplicable intrinsic dynamics exhibited by the neurons at multiple timescales is only a little understood and hence there is a growing need to study the dynamics of the neuronal activity. In this project, we investigate the plausibility of characterising these neuronal activities into regular and chaotic regimes by the magnetic resonance of spins in the neuron cell walls.

Contents

Chapter 1

Introduction

The research on the chaotic attributes of neurons led to the discovery of chaos in the brain and established the study of brain activity in the framework of non-linear dynamics [1]. In the past decade, we have seen an increased study focusing on the dynamics of the neuronal activity that we are now able to define as a deterministic dynamical phenomenon.

At present, there exists two non-invasive techniques that are being used to map and study the neuronal activity. However, these techniques are known to be efficient only in either the temporal or spatial domain. Functional magnetic resonance imaging (fMRI) measures brain activity by detecting the change in blood flow. Even though this technique is known to have a good spatial resonance, fMRI's temporal resolution is limited by its hemodynamic response time. In contrast to this, Electroencephalography (EEG) measures the electrical activity generated by neurons, providing excellent high temporal but poor spatial resolution.

The functioning of the neurons can be classified into regular or chaotic regimes. Some researches have shown that the dynamics of spin systems submitted to noisy signals present signatures of the nature of those noises [2]. Hence, the magnetic resonance of spins in a neuron cell wall may give rise to some interesting characteristics that will enable us to classify the neuronal activity modes. The objective of this project is to test this hypothesis. In order to do so, we simulate a spin ensemble with no mutual interactions in the presence of electromagnetic and thermal noises.

The remainder of this paper is organised as follows; Chapter 2 describes the evolution of a quantum spin ensemble at magnetic resonance. In Chapter 3, we study the magnetic resonance of a spin ensemble submitted to the electromagnetic noises modelled by the Fitzhugh-Nagumo and the Hindmarsh Rose models. Chapter 4 deals with the interaction of the spin ensemble with thermal noises and Chapter 5 presents the results for the simulation of the spin ensemble submitted to all three interactions: with the MRI external magnetic field, with the chaotic electromagnetic noises and with the thermal noises from the biological media. In Chapter 6, we present an epistemological study based on this subject and finally in Chapter 7, we summarise the results of this paper.

In this project, we also observe the interplay between a classical dynamical system, represented by the thermal and electromagnetic noises, with a quantum system, which is the spin ensemble. There is growing evidence that the future study of neuronal activity and its relation to higher brain functions will be a combination of the study of classical and quantum systems.

For the theoretical review, we have not chosen a particular unit system for defining the equations, whereas for the simulations, we mainly choose atomic units unless to test some special cases.

Chapter 2

Magnetic Resonance of the spin ensemble

Nuclear Magnetic Resonance (NMR) is one of the most widely used techniques to probe into the structures of certain nuclei. This technique is used to measure magnetic fields at high precision. It is a physical phenomenon associated with the intrinsic angular momentum of the spin and the magnetic properties of atomic nuclei [3]. When the spin ensemble is exposed to a constant magnetic field and perturbed with an oscillating electromagnetic field, we observe magnetic resonance which is a quantum mechanical resonance effect. In this chapter, we review the dynamics of the evolution of the spin ensemble in the presence of such a magnetic field.

2.1 Dynamics of the spin ensemble

We consider an ensemble of N spins without the spin-spin interactions. Every spin will have a time dependant Hamiltonian as given in equation 2.1 and the evolution of the spins is known to obey the Schrödinger equation.

$$i\hbar\dot{\psi}_i(t) = H(t)\psi_i \tag{2.1}$$

For the evolution of the Schrödinger equation, we use the split operator method (refer, A.3.2). Hence, states with definite energy evolve in time with the operator $e^{-i\hbar^{-1}H(t_n)\Delta t_n}$. At the initial time t = 0, all the spins are in the same quantum state and thus completely coherent with each other, given by $\psi_i(0) = \psi_0$. We make an arbitrary choice that all the spins are in the Schrödinger cat state ($|\alpha|^2 + |\beta|^2 = 1; \alpha, \beta \neq 1$) such that at t = 0 we have

$$|\psi_0\rangle = \alpha\,|\uparrow\rangle + \beta\,|\downarrow\rangle \tag{2.2}$$

The quantum Hamiltonian of a single spin with only the presence of the MRI magnetic field is given by $H_0 = \gamma(\mathbf{B} \cdot \mathbf{S})$, where $\mathbf{S}$ is the Pauli matrices and the constant of propotionality γ is called the gyromagnetic ratio. The magnetic fields will be assumed to be of the form

$$\vec{B} = B_0\hat{\mathbf{i}} + B_1(cos(\omega t)\hat{\mathbf{j}} - sin(\omega t)\hat{\mathbf{k}}) \tag{2.3}$$

Due to the application of the magnetic field, the spins in the spin ensemble will execute a wobble like motion about the z axis. This is called precession and it corresponds to the gyration of the rotating axis of a spinning body about an intersecting axis.

In equation 2.3, B_0 is the primary magnetic field in the z-direction, B_1 is the very weak perturbing field strength and ω is the frequency of the perturbation, also known as the larmor frequency. This is the resonant frequency or the precessional frequency and is proportional to main field strength. It is represented as $\omega = \gamma B_0$.

At t > 0, the spin ensemble is submitted to different noises that will modify the quantum Hamiltonian of the i^{th} spins. Then, we can represent the state of the i^{th} spin undergoing a temporal evolution as

$$|\psi_{n+1}^{(i)}\rangle = U_n^{(i)} |\psi_n^{(i)}\rangle \tag{2.4}$$

Here, U is the evolution operator. The quantum mechanical wave function can only describe a pure system, so instead we find the density matrix, which is a better choice to measure macroscopic quantities such as magnetic fields, as its capable of quantitatively describing physical situations with mixed as well as pure collections. The density matrix of the spin ensemble is represented by

$$\rho_n = \frac{1}{N} \sum_{i=1}^{N} |\psi_n^{(i)}\rangle \langle\psi_n^{(i)}| \tag{2.5}$$

The density matrix encodes two fundamental piece of information. The average probabilities of the occupation of the given states can be obtained from the density matrix by calculating $\langle\uparrow|\rho|\uparrow\rangle$ for the probability of spins in the up state and $\langle\downarrow|\rho|\downarrow\rangle$ for the probability of spins in the down state. Moreover, the coherence of the states can be found from $\left|\langle\uparrow|\rho|\downarrow\rangle\right|$. A decrease in this value of the coherence would indicate a decoherence phenomenon. Initially, when all the states are in the same quantum state, we have maximum coherence indicating a quantum superposition. On the other hand, if the value of the coherence is 0, we have some spins in the state $|\uparrow\rangle$, while the others are in the state $|\downarrow\rangle$, indicating that the bath is a classical mixture of spins.

The changes that have been invoked in the system after its interaction with noises is shown in the variation of the measured macroscopic quantity, the magnetic field. The emitted magnetic field of the spin is given by

$$\mathbf{B} = \gamma tr(\rho \mathbf{S}) \tag{2.6}$$

Hence, by visualizing the changes in the density matrix (ρ), we can study the fluctuations in the emitted magnetic field, if there are any present.

Chapter 3

Interaction of the spin ensemble with electromagnetic noise issued from neuronal activity

The exceeding complexity of the nervous system requires innumerable equations to understand its working. However, some principle properties of the neurons such as its electrical activity have been the main focus of several researches which has led to the development of several models established to study its properties.

Since the pioneering works of Hodgkin and Huxley [4], a large number of models that describe the electrical activities of the neurons have been developed; the two dimensional FitzHugh Nagumo model and the three dimensional Hindmarsh-Rose model are the simplest and highly efficient of these models.

In this chapter, we model the electromagnetic noises issued from the neuronal activity using the above mentioned simple classical dynamical systems and simulate the dynamics of the quantum spin ensemble submitted to these noises.

3.1 Interaction Hamiltonian

For t > 0 the spin ensemble is submitted to the electromagnetic noises. When the spins in the cell membrane interact with these chaotic noises generated from the electrical activities of the neurons, the quantum Hamiltonian of the i^{th} spin is modified by the addition of an interaction potential $V_{int}(t)$ given as

$$H^{(i)}(t) = H_0(t) + V_{int}(t) \tag{3.1}$$

This interaction potential can be modelled in many ways. For this simulation, we model it as $V_{int}(t)$ = $\mathbf{E} \cdot \mathbf{S}$. Then, the final interaction Hamiltonian governing the magnetic resonance of the spin dynamics is represented as

$$H^{(i)}(t) = \gamma(\mathbf{B} \cdot \mathbf{S}) + \epsilon(\mathbf{E} \cdot \mathbf{S}) \tag{3.2}$$

Here, ϵ is the coupling constant for the electromagnetic fields due to the neuronal activity. This is given by $\epsilon = \mu_0 \mathbf{B}$. The ratio of the coupling constants γ and ϵ is varied to control the transition between the classical and quantum dynamics.

To model the chaotic characteristics of the electromagnetic noises, we choose N initial conditions ($N\{x_0^{(i)}\}_{i=1,...,N}$) from a Gaussian distribution such that

$$\mathbf{E} = f_{\vec{x_0^{(i)}}}\Big(x(t), y(t), z(t)\Big) \tag{3.3}$$

The variables $x(t), y(t), z(t)$ are chaotic variables generated at the chaotic regimes of the models dealt with in the upcoming sections 3.2 and 3.3.

3.2 FitzHugh-Nagumo model

The FitzHugh-Nagumo model (FHN) is a two dimensional reduced and simplified generic model of the excitable neuron media created from the famous Hodgkin-Huxley model. FHN is one of the most intensively studied chaotic models of neuronal activity [5] due to its simplicity. It is mathematically expressed in terms of two polynomial differential equations given below

$$\begin{aligned} \dot{x} &= x(x-1)(1-\alpha x) - y + I_0(t) \\ \dot{y} &= bx \end{aligned} \tag{3.4}$$

Here, $I_0(t)$ represents the external stimulus and is given by $I_0(t) = \frac{a}{\omega}cos(\omega t)$, where a and ω are the amplitude and the frequency of the applied electromagnetic field respectively, where $\omega = 2\pi f$, f being the frequency of the stimulus. For the parameter values: α = 10, b = 1, a = 0.1 and f = 0.1271, the FHN system shows a chaotic attractor in the phase space as depicted in figure 3.1. We will use these chaotic variables for the addition of electromagnetic noise to the system.

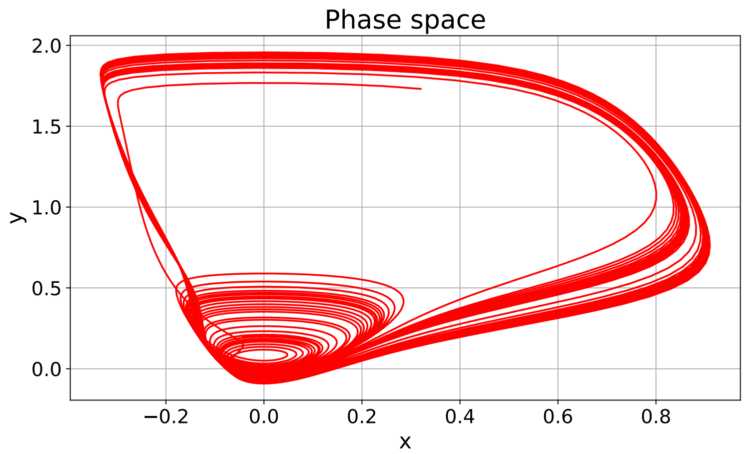

FIGURE 3.1: Phase space of FitzHugh-Nagumo chaotic attractor

We model the dynamics of the evolution of density matrix, in the presence of electromagnetic noise, by the addition of chaotic variables x and y. Initially, we simulate the system for values of coupling constant γ equal to the electromagnetic field coupling constant ϵ, taken in atomic units. We have N = 10, initial conditions taken from a Gaussian distribution between -1 and 2 for a magnetic field (B_0) of strength 10^{-5} a.u.

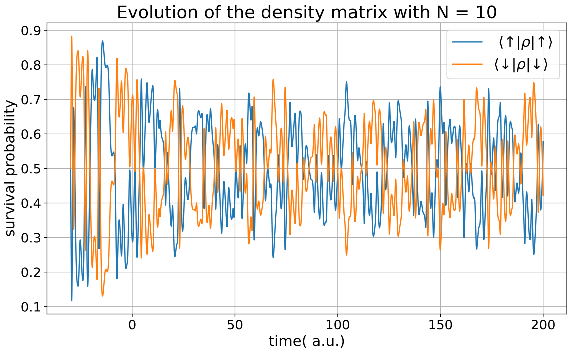

(A) Evolution of population

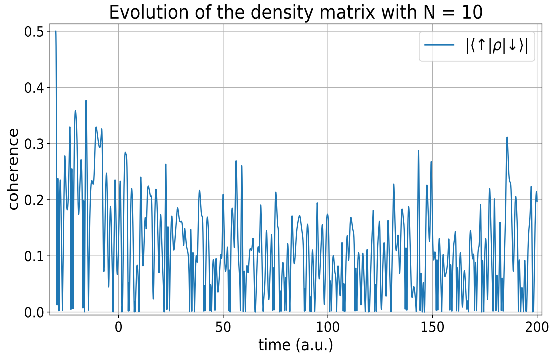

(B) Evolution of coherence

FIGURE 3.2: Evolution of density matrix by addition of noises from the FitzHugh-Nagumo model for 10 initial conditions and $\gamma = \epsilon$

Figure 3.2a shows the probability of finding the spins in either the up or down states. For a simulation with equal coupling constants, we observe that the survival probability average out to 0.5 due to the rabii oscillations. As the coherence of spins dropped to zero and fluctuate around this value, the population also averages out to 0.5 with high fluctuations.

We find that the relaxation of the survival population in not present. The regularity of the FitzHugh-Nagumo model that shows only little chaotic presence is the reason for this absence of relaxation. The relaxation processes are induced by the effect of noises onto the system and due to the overly simple nature of this dynamical system, it is not possible to observe this relaxation. Thus, all the states of the population remains in their initial state and only highly fluctuate around the average value of 0.5.

In figure 3.2b, due to the extremely fast oscillations it seems to be not possible to observe a plateau for the decoherence. The decoherence happens almost immediately after the beginning of the simulation and fluctuates highly around zero due to the low value of N. We can assume that the plateau during the beginning of the decoherence is only observable when the Lyapunov exponents for the evolution of the quantum system is of the same order as that of the time scale chosen for evolution. Here on the other hand, we assume that the Lyapunov exponents are much larger than the quantum oscillations making it impossible to observe the plateau for decoherence due to chaos.

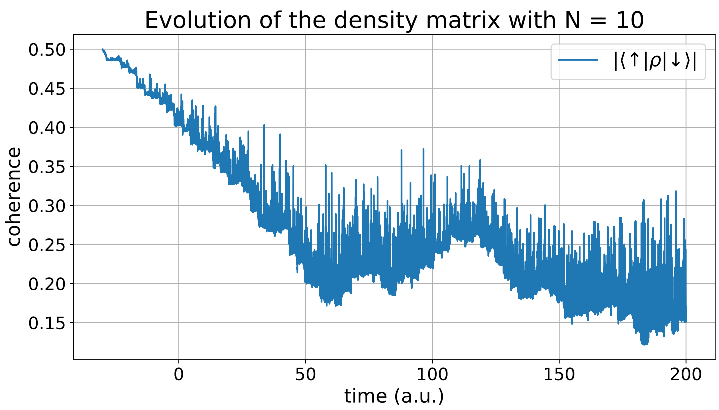

FIGURE 3.3: Evolution of coherence for N = 10 initial conditions and $\epsilon > \gamma$.

It is possible to choose the time-scales of classical and quantum evolution by adjusting the coupling parameters. Even though this does not model realistic environment for neuronal activity, it is interesting to observe a case where we choose $\epsilon > \gamma$, such that $\epsilon = 10^5\gamma$. This is depicted in figure 3.3. We observe that on increasing the coupling factor ϵ, the time for the decoherence of spins has increased and instead of a rapid drop, there is a rather slow decline. Finally, we study the system for N = 100 initial conditions, where we observe an averaging of the fluctuations making the decoherence process more visible as compared to Figure 3.2a and 3.2b. We also validate that the further increase of the value of N do not produce significant changes in the system due to its averaging properties.

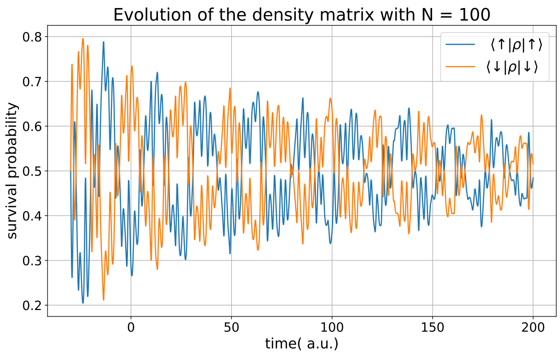

(A) Evolution of population for $\epsilon = \gamma$

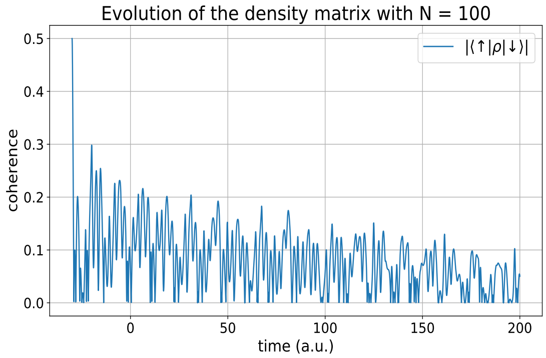

(B) Evolution of coherence for $\epsilon = \gamma$

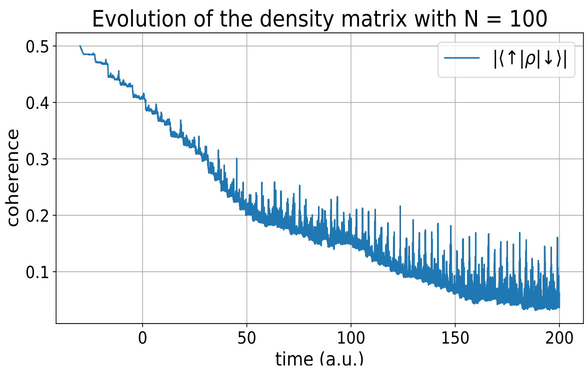

(C) Evolution of coherence for $\epsilon > \gamma$

FIGURE 3.4: Evolution of density matrix by addition of noises from the FitzHugh-Nagumo model for 100 initial conditions

3.3 Hindmarsh-Rose model

The Hindmarsh-Rose neuronal model (HR) is a simple model that is able to produce the spiking properties of the neurons. Similar to the FitzHugh-Nagumo model, this is also a simplification of the Hodgkin-Huxley model into three dimensions. This model is also able to represent the chaotic bursting dynamics [6] of the neurons that is based on external stimulus. The HR model is described by the following system of differential equations:

$$\begin{aligned}\frac{dx}{dt} &= \frac{1}{\tau_x}(-\tau_x x + y - ax^3 + bx^2 + z)\\ \frac{dy}{dt} &= -ax^3 - (d-b)x^2 + z\\ \frac{dz}{dt} &= \frac{1}{\tau_z}(-sx - z + c)\end{aligned} \tag{3.5}$$

The system is known to show chaotic behaviour for the parameter values: τ_x = 0.03, τ_z = 0.8, a = 0.49, b = d = s = 1.0 and c = 0.0322. The phase space and the evolution of the dynamical system in time is illustrated in the figure 3.5. Unlike the previous model, now we have three chaotic variables x, y and z that will be added to the interaction Hamiltonian.

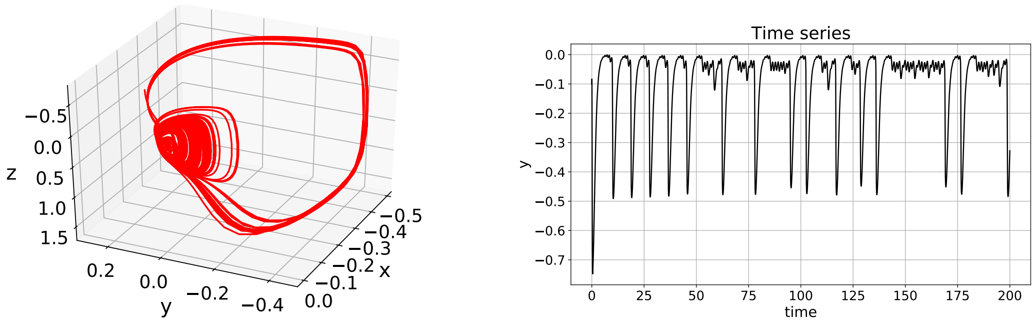

(A) Phase space diagram (B) Time series

FIGURE 3.5: Hindmarsh-Rose chaotic attractor

We simulate the dynamics of the spin ensemble submitted to the three dimensional electromagnetic noises for a period of 5000 a.u for N = 10 initial conditions. We make a choice that the coupling constants are equal and the magnetic field strength B_0 is equal to 10^{-5} a.u.

The behavior of the spin ensemble is then slightly different to that of a spin ensemble submitted to electromagnetic noises generated using the FitzHugh-Nagumo model. In the previous system, we were unable to observe the relaxation effects on the spin ensemble due to the effect of noises. Here, on the other hand, due to the highly chaotic ature of the Hindmarsh-Rose model, we observe the relaxation processes leading to a population jump.

Figure 3.6a depicts that after around 1000 a.u., the coherence falls rapidly to zero and there is a population jump in the figure 3.6b. Towards the end of the evolution of the system, the spin ensemble is almost completely in the spin up state although they were initially in a Schrödinger state with about 50% of the population was in the spin up state $|\uparrow\rangle$ and the other 50% in the spin down state $|\downarrow\rangle$. Thus, we observe an evolution of the population to a value different from its initial state. Such population jumps were not visible in section 3.2 due to the strong influence of rabii oscillations onto the system. We also notice that the relaxation is a long term process.

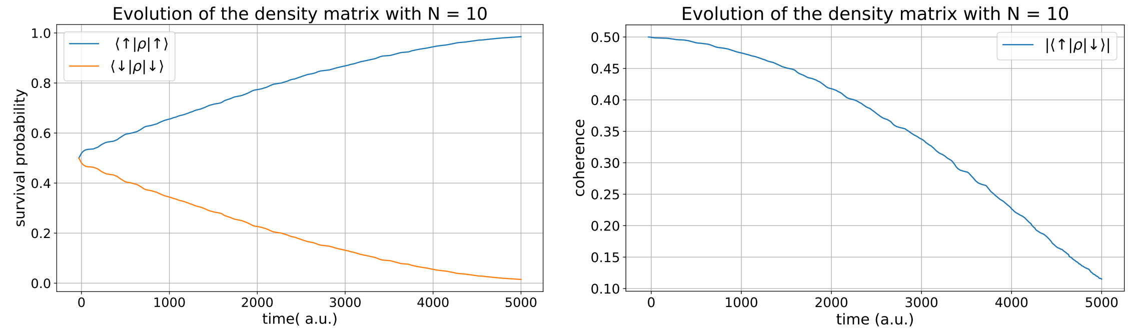

(A) Evolution of the population

(B) Evolution of Coherence

FIGURE 3.6: Evolution of the density matrix by addition of noises from Hindmarsh-Rose model for $\gamma = \epsilon$

The arbitrary choice of Schrödinger cat state for the initial states of the spins ensures a strong distribution of spins throughout the phase space. The decoherence process is accounted to this dispersion and thus every spin views the field differently and evolves with different amplitudes leading to a loss of coherence with temporal evolution.

Chapter 4

Interaction of the spin ensemble with thermal noises

The neurons in the brains are not isolated systems, instead they are continuously interacting with the biological environment. One of the chief sources of stochastic variability on the cellular level is the effect of temperature on the system. Many sources of the electromagnetic noises are affected by the temperature of the source and the environment. Hence, thermal noises are intrinsic to any system operating above zero Kelvin. The effect of these thermal noises onto the spins is modelled using the Optical Bloch equations (OBE). OBE describes the coherent exchange of energy between a quantum system such as the spin ensemble and a magnetic field in the presence of thermal noises. In this section, we deal with the macroscopic magnetization vector since we can consider spins as quantum magnetization vectors up to a given multiplicative constant.

4.1 Bloch Equations

We consider a spin ensemble that is incoherent at time t = 0. We make an assumption that they have different resonant outsets ω varying in amplitude α, which is just a coupling constant. The dynamics of the magnetization vector or the extended Bloch vector, $\vec{M} = (1, M_x, M_y, M_z)^t$ is governed by the Bloch matrix [7]. In a rotating frame, the equations are given as

$$\frac{d}{dt}\vec{M} = \begin{pmatrix} 1 & 0 & 0 & 0 \\ 0 & -\frac{1}{T_2} & -\omega & \alpha\omega_y(t) \\ 0 & \omega & -\frac{1}{T_2} & -\alpha\omega_x(t) \\ \frac{1}{T_1} & -\alpha\omega_y(t) & \alpha\omega_x(t) & -\frac{1}{T_1} \end{pmatrix} \vec{M} \tag{4.1}$$

To normalise the radius of the Bloch sphere to 1, we have a four vector representation. $M^{(\omega)}_{x,y,z}$ is the coordinates of the magnetization vector in the x, y and z directions. T_1 and T_2 are relaxation times due to the interaction between the spins with their biological environment. ω_y and ω_x are the amplitudes of the control fields. The control fields in this case are defined as a series of short dirac pulses.

We integrate the system of Bloch equations using the matrix exponential method. Due to this choice of integrator, it is not possible to study the dynamics of the magnetization vectors in atomic units and instead we calculate this in classical units. However, it is possible to assume an artificial environment where T_1 and T_2 values are chosen to be of higher values than what is induced in the biological media such that $1/T_1$ and $1/T_2$ are very small values. In this simulation however, we assume that T_1 = 0.2 s and T_2 = 0.3 s.

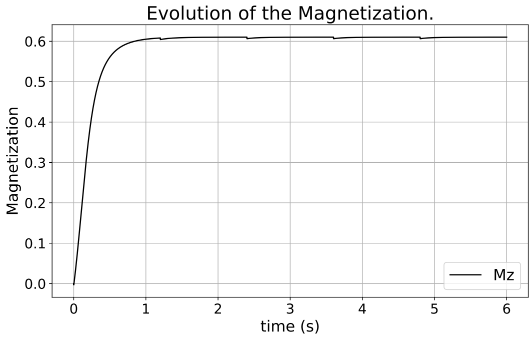

(A) Magnetization vector in z direction.

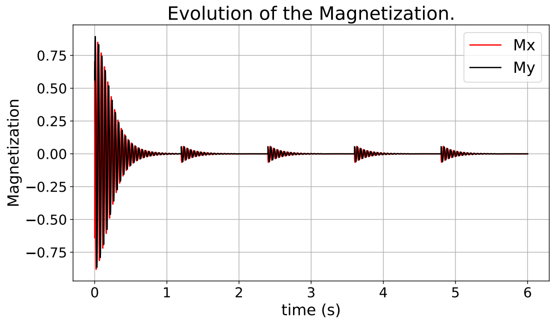

(B) Magnetization vector in x and y direction.

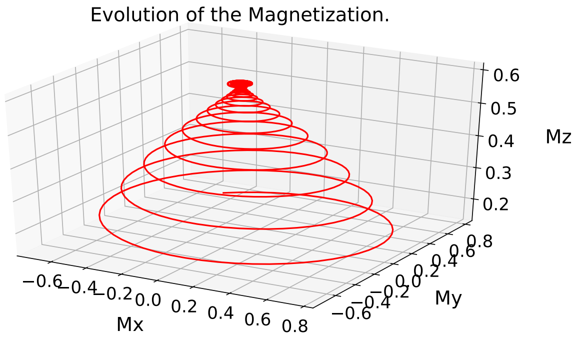

(C) Precession of $\vec{M}$ around the z axis

FIGURE 4.1: Evolution of the Magnetization vector.

The dynamics of the magnetization vector is show in figure 4.1. The magnetization vector similar to the density matrix, shows the collective behaviour of many spins given by

$$\mathbf{M} = \alpha tr(\rho \mathbf{S}) \tag{4.2}$$

Here, α is a constant accounting for the averaged property of magnetization. T_1 relaxation time acts as a decay constant for the recovery of the $\hat{\mathbf{z}}$ component of the Magnetization vector $\vec{M}$. In figure 4.1a, this component is seen to decay towards a thermal equilibrium value of the magnetization (M_{zeq}) around 0.6.

The consideration of an inhomogenous magnetic field presents interesting results in the decay of the magnetization vector. Spins precess at a different rate in different regions due to this inhomogenity in the static magnetic field $\mathbf{B_0}$. This leads to the phase differences and hence a quicker loss of the averaged transverse magnetization. However, even after the decay of the transverse magnetization components, we are able to recover the amounts that has been lost during relaxation. This is depicted in the figure 4.1b and this phenomenon is referred to as the spin echo. Finally, figure 4.1c, illustrates the clockwise Larmor precession of $\vec{M}$ about the z-axis.

Chapter 5

Interaction of the spin ensemble with thermal and electromagnetic noises

In the final part of the simulation, we study the dynamics of the spin ensemble submitted to an interaction with all three components: with the external magnetic field of the MRI (see, Chapter 2), with the chaotic electromagnetic noises (see, Chapter 3) issued from the neuronal activity and with the thermal noises (see, Chapter 4) for the interaction with the biological medium.

5.1 Evolution of Magnetization

The evolution of the magnetization vector in presence of both electromagnetic and thermal noises is modelled by a modification in the Bloch equations as given in equation 5.1, similar to Chapter 4.

$$\frac{d}{dt}\vec{M} = \begin{pmatrix} 1 & 0 & 0 & 0 \\ 0 & -\frac{1}{T_2} & -\omega + \epsilon f(z(t)) & \alpha\omega_y(t) + \epsilon f(y(t)) \\ 0 & \omega + \epsilon f(z(t)) & -\frac{1}{T_2} & -\alpha\omega_x(t) + \epsilon f(x(t)) \\ \frac{1}{T_1} & -\alpha\omega_y(t) + \epsilon f(y(t)) & \alpha\omega_x(t) + \epsilon f(x(t)) & -\frac{1}{T_1} \end{pmatrix} \vec{M} \quad (5.1)$$

Here, the electromagnetic noises $\vec{f}_{x_0^{(i)}}\Big(x(t), y(t), z(t)\Big)$ are added to the Bloch equations by choosing that $\alpha = \gamma$.

5.2 Interactions with two dimensional chaotic electromagnetic noises

In this section, we have added the two dimensional chaotic variables $x(t)$ and $y(t)$ generated by the FitzHugh-Nagumo model with $z(t)$ equal to zero accounting to no addition of noises in the z direction. The FitzHugh-Nagumo model is periodic in the phase space and hence when it is coupled with the thermal evolution of magnetization, it does not bring about a huge change in the trajectory of the evolution of magnetization.

The final trajectory of the evolution of magnetization depicted in figure 5.1c, remains unchanged since the spin dynamics are mainly based off the coherence and decoherence of the spins. This accounts to the fact that the thermal noises dominate the evolution of

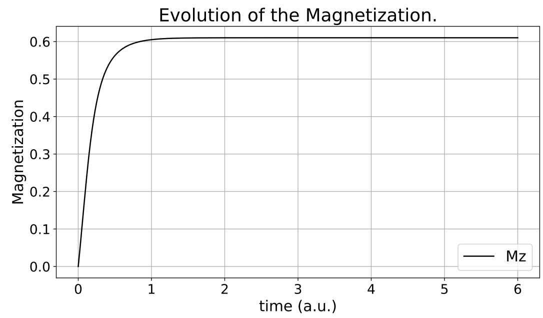

(A) Magnetization vector in z direction.

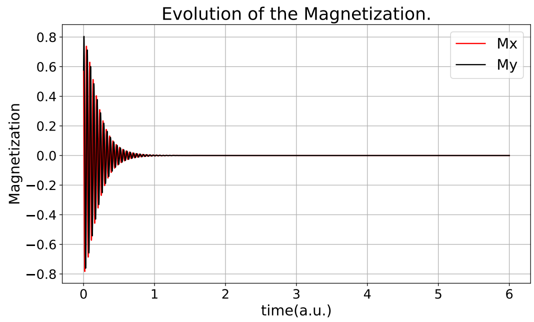

(B) Magnetization vector in x and y direction.

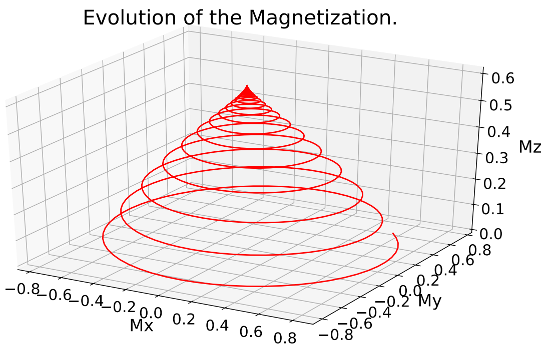

(C) Precession of $\vec{M}$ around the z axis

FIGURE 5.1: Evolution of the Magnetization vector after the addition of chaotic electromagnetic noises from the FitzHugh Nagumo model for coupling constants $\gamma = \epsilon$

the system and chaotic noises show almost no effect on the final trajectory of the evolution of $\vec{M}$. Thus, in realistic time scales, it is not possible to detect the presence of such chaotic noises issued from neuronal activity due to it's shadowing by the interaction of the neurons with biological medium acti

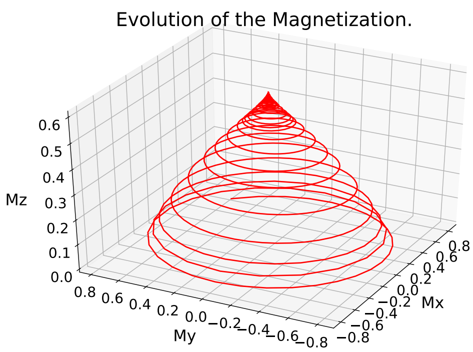

(A) $\epsilon = 10^8\gamma$

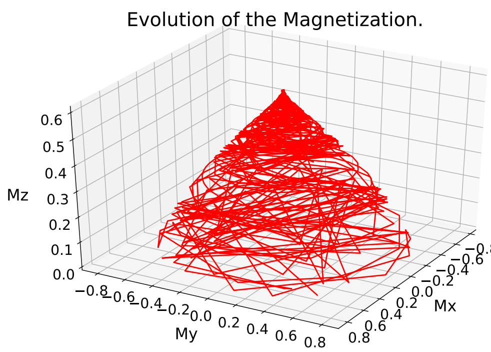

(B) $\epsilon = 10^9\gamma$

FIGURE 5.2: Evolution of $\vec{M}$, modelled with a high value for ϵ

The only noticeable change in the evolution of the system is the removal of echos that are generated due to the inhomogenity of the electromagnetic field on the addition of noises.

The decay of the transverse and longitudinal magnetization is made smoother due to the fact that the coupling amplitudes of the control pulses and that of the electromagnetic noises are almost the same. This will lead to masking the observation due to an increased relaxation time.

For the qualitative analysis of the problem, we can assume an artificial biological environment with a high value of the electromagnetic coupling constant ϵ to see the effects of the chaotic noises onto the system. We increase the value of the coupling constant ϵ, to observe the chaotic evolution of the Magnetization vector $\vec{M}$ in the phase space.

From the figure 5.2, we observe that for a value of ϵ greater than $10^8\gamma$, we can see the effects of the chaotic noises. The evolution of the magnetization vector $\vec{M}$, is extremely chaotic for a choice of $\epsilon = 10^9\gamma$. However, this modelling is not useful for studying the dynamics of neuronal activity in real time scales and we can conclude that the detection of chaotic noises is nearly impossible in the presence of a biological medium with high temperature. It could almost only be detected if there were a possibility to control the temperature of the biological medium and bring it down to very low temperatures.

5.3 Interactions with three dimensional chaotic electromagnetic noises

We add the chaotic variables $x(t)$, $y(t)$ and $z(t)$, generated from the dynamical Hindmarsh-Rose model described in section 3.3.

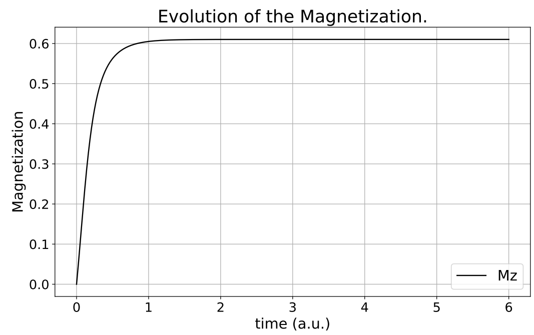

(A) Magnetization vector in z direction.

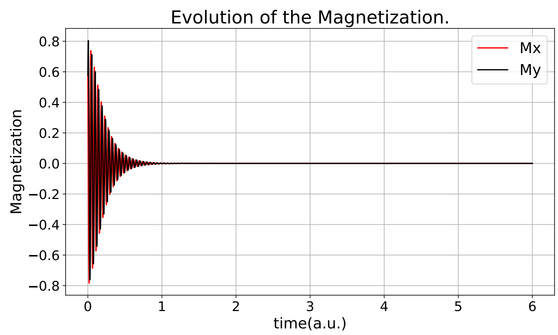

(B) Magnetization vector in x and y direction.

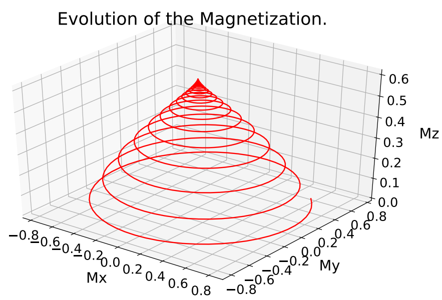

(C) Precession of $\vec{M}$ around the z axis

FIGURE 5.3: Evolution of the Magnetization vector after the addition of chaotic electromagnetic noises from the Hindmarsh-Rose model for coupling constants $\gamma = \epsilon$

There is an addition of electromagnetic noises onto all the three components of the magnetization vector ($\vec{M}$). However, in figure 5.3, as in the case of the addition of noises from the FitzHugh-Nagumo model, we notice that the trajectory remains unchanged.

Hence, we once again simulate the evolution of the magnetization vector in an artificial environment with high electromagnetic coupling constant ϵ. We realise that for a value of epsilon greater that $\epsilon = 10^6\gamma$, the effects of the chaotic noises is visible in the evolution of the magnetization vector, modifying its final trajectory. The evolution of the magnetization vector for two values of epsilon, $\epsilon = 10^6\gamma$ and $\epsilon = 10^7\gamma$ is illustrated in the figures 5.4 and 5.5.

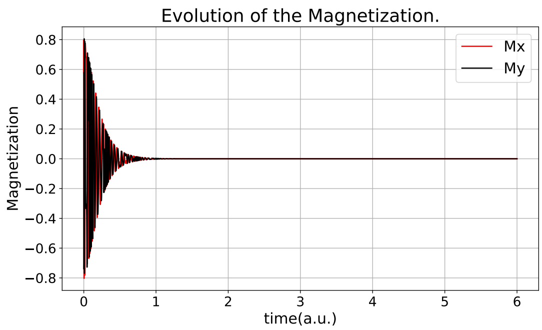

(A) Evolution of magnetization vector in the x and y axis

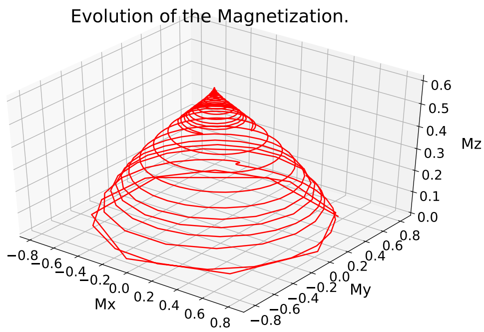

(B) Evolution of Magnetization vector.

FIGURE 5.4: Evolution of the Magnetization vector after the addition of chaotic electromagnetic noises from the Hindmarsh-Rose models for $\epsilon = 10^6\gamma$

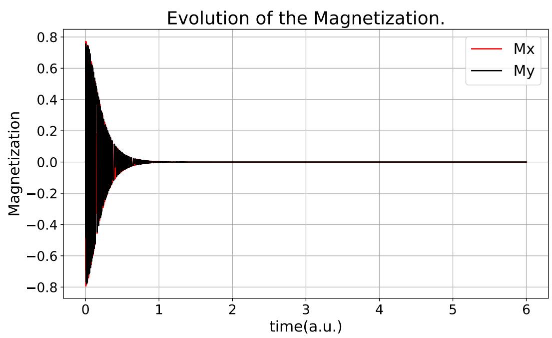

(A) Evolution of magnetization vector in the x and y axis

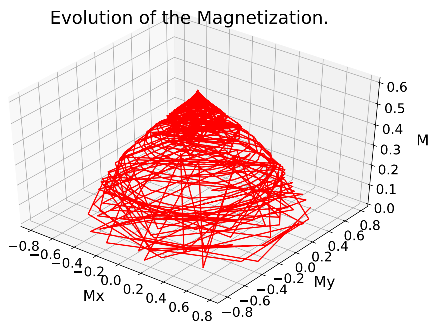

(B) Evolution of Magnetization vector.

FIGURE 5.5: Evolution of the Magnetization vector after the addition of chaotic electromagnetic noises from the Hindmarsh-Rose models for $\epsilon = 10^7\gamma$

We observe that the influence of the chaotic noises on the system is more evident at higher values of the electromagnetic coupling constant ϵ. Moreover, since there is an addition of three chaotic variables by the noises generated from the Hindmarsh-Rose model as compared to only two variables from the noises generated by the FitzHugh-Nagumo model, it is possible to observe the effect of the electromagnetic chaotic noises at a lower values of ϵ such as $\epsilon = 10^6\gamma$ for the Hindmarsh-Rose model instead of $\epsilon = 10^8\gamma$ for the FitzHugh-Nagumo model.

Chapter 6

Epistemological Study

6.1 Predicting Brain Patterns

Decoding and analysing massive amounts of data remains to be a major problem limiting several advancements in technology. This data is not often ordered but instead might be inter-wined, chaotic and disordered similar to biological information from the environment. Hence, decoding the information processing abilities of the brain, could lead to massive advancements in data processing and analysis. For this, it is important to consider the brain as a dynamical system that is continually interacting with the environment and invoking change. Recent studies have shown that by studying the functioning of the brain in regimes where it transitions from the regular to the chaotic [8] could give us more insight into why the brain works the way it does and the patterns behind brain functioning.

6.2 Quantum Consciousness

Recent researches in psychology and cognitive neuroscience have shown that the application of nonlinear dynamics, chaos and self-organization seem to be particularly important for research of some fundamental problems regarding mind-brain relationship [9]. Our knowledge about the subjective nature of the conscious mind remains limited. There is a raging debate on the link between consciousness and quantum mechanics. Roger Penrose, a British physicist, proposed in his book, The Emperor's mind [10], that our ability to sustain seemingly incompatible mental states is no quirk of perception but a real quantum effect. However, when a quantum object interacts with nature, the quantum effects such as superposition is destroyed and the quantum nature is slowly lost due to the process of decoherence. Especially in environments of high temperature, the decoherene process is known to be very rapid and the timescales for decoherence [11] between the classical and quantum states play a major role.

Understanding the functioning of the human brain in the context of quantum mechanical ideas and chaos serve as an important link to probing into the mysteries of consciousness. Hence, the study of the dynamics of the spin system in a high temperature biological environment also accounting for the neuronal electromagnetic noises plays an important role in evaluating the decoherence nature of a system that attempts to transition between the classical and quantum regimes. This project opens up new research ideas that hopes to one day understand the link between the mind and the brain.

6.3 Development of Artificial Intelligence

Beyond decoding neural networks and its functioning, the ideas proposed in this paper can be applied to variety of other projects such as an advancement in the field of artificial intelligence that could mimic the greatest computer known to human kind, the brain. Machine learning tasks that are designed to run algorithms similar to brain functioning requires high amount of computing power unlike the efficiency at which the brain computes these tasks. Nowadays, we witness an increased study of the dynamics of functioning of neurons that aims to improve the efficiency of software and algorithms related to the functioning of biological systems. The synapses in the neurons only function at temperatures close to absolute zero [12] and hence the study of the effects of the thermal noises onto the neuronal activity is very important in order to control the activity at higher temperatures.

Chapter 7

Conclusion

This work is motivated both by an intellectual goal of creating a model for the dynamics of the neuronal activity that better analyzes the chaotic behaviour of the brain activities as well as the related goal of understanding the importance of such researches for future advancements in the field of neuroscience such as finding the missing link between the mind and the brain, and even the development of computational devices as powerful and efficient as the brain.

Such projects are in desperate need of strong theoretical framework to find solutions to the problems that have been proposed. The lack of knowledge in several interdisciplinary fields accompanying this work allows us to only provide a qualitative analysis of the problem rather than a quantitative analysis. The simulations conducted are limited by the vast amounts of assumptions taken into consideration to simplify the problem in hand when the true complexity of studying the nature of brain functions looms over the reliability of the results produced.

Within the framework of a controlled simulation modelling the dynamics of the spins in a neuron cell wall, we can conclude that it is not possible to detect the effects of chaotic electromagnetic noises issued from neuronal activity, on the system studied due to the rapid decoherence of the system from its interaction with the environment. Hence, this also disproves the plausibility of characterising the neuronal activity into different activity modes such as regular and chaotic at realistic time-scales of the functioning of the brain.

This program is only a first step that simulates the simple dynamics of the neuronal activity. The realisation of this project has made us aware of the need to control the fall of coherence in such quantum systems. Future works can be focused on increasing the relaxation time for decoherence such that there is a longer period or an evident plateau before the fall of the coherence value to zero. This can be performed by choosing different trajectories in the phase space of the external magnetic field and the search for a regime where we are able to observe a slow fall in this decoherence value. It is not conceivable to realise these steps in the time period of this internship.

It is therefore, still unclear whether or not a simple program could articulate the proposed theories given its inherent complexities. While many questions remain unanswered, the next few years will likely see a revolution in the study of such interfaces between classical and quantum systems as tools from mathematics and complex systems, which have as of now only brushed the surface of this infinitely complex field of chaos in neuroscience.

Appendix A

Technical Report

End of Development Date: 24^{th} June, 2021

Programming Language: Python 3

A.1 Goal of the Program

The goal of this project is to develop a simulation for the dynamics of a spin ensemble (spins in a neuron cell wall), submitted to three interactions: magnetic resonance from the MRI, electromagnetic noises issued from neuronal activity and with the biological medium acting as a thermostat.

A.2 List of Files

init.py
integrator.py
dynamical_sys.py
schrodinger.py
electromagnetic_noises.py
functions_thermal.py
thermalnoises.py
electric+thermal.py

A.3 Integrators

A.3.1 Runge Kutta Fourth Order Algorithm

To approximate the solution to a first order differential equation such as

$$\frac{dy(t)}{dt} = \dot{y}(t) = f(y(t), t) \qquad \text{where, } \; y(t_0) = y_0 \tag{A.1}$$

where $y \in \mathbb{R}^n$ and $F : \mathbb{R}^n \to \mathbb{R}^n$ (F is not a linear map). We denote by y^i, the i-th component of y and by $F^i(y)$ the i-th component of the image of y by F.

T is the time on which we want to simulate the system such that $\Delta t = \frac{T}{N_t}$ be the step of the simulation ($N_t \in \mathbb{N}$ is total number of steps in the simulation). The time dependence is then modelized with the time partition $\{t_0, t_1, \ldots, t_{N_t}\}$ with $t_n = n\Delta t$.

Let $y_n \equiv y(t_n)$, be the value of the vector y at time t_n. Then RK4 integrator for the first order differential equations are based on the definition of the derivative:

$$\dot{y}(t_n) = \lim_{h\to 0}\frac{y(t_n+h)-y(t_n)}{h} \simeq \frac{y_{n+1}-y_n}{\Delta t} \tag{A.2}$$

with Δt sufficiently small (N_t sufficiently large, the time partition sufficiently thin).

We begin with some initial conditions, $y(t_0) = y_0$. The development of the Fourth Order Runge-Kutta method closely follows that of the Second Order Runge-Kutta. We use four approximations to the slope at some time t = 0. There is a refinement to estimate F at the middle point. Its propagation scheme is

$$y_{n+1} = y_n + (K_{1,n} + 2K_{2,n} + 2K_{3,n} + K_{4,n})\frac{\Delta t}{6} \tag{A.3}$$

with, the four approximations onto the slope given by

$$\begin{aligned} K_{1,n} &= F(y_n) \\ K_{2,n} &= F(y_n + K_{1,n}\frac{\Delta t}{2}) \\ K_{3,n} &= F(y_n + K_{2,n}\frac{\Delta t}{2}) \\ K_{4,n} &= F(y_n + K_{3,n}\Delta t) \end{aligned} \tag{A.4}$$

A.3.2 The Split Operator Method

The split operator algorithm is based on the group rule of the evolution operator:

$$U(T, t_0) = U(t_N, t_{N-1})U(t_{N-1}, t_{N-2})\ldots U(t_1, t_0) \tag{A.5}$$

On a small duration Δt, the time ordered exponential is almost equal to a matrix exponential:

$$U(t_{n+1}, t_n) \simeq e^{-i\hbar^{-1}H(t_n)\Delta t} \tag{A.6}$$

The propagation scheme is then:

$$\psi_{n+1} = e^{-i\hbar^{-1}H(t_n)\Delta t}\psi_n \tag{A.7}$$

The computation of the matrix exponential can be realized by using some numerical computation libraries. The quality of the approximation depends on the method used to compute the exponential. The algorithm is unconditionally stable, that is to say it converges for all Δt (this does not mean that it converges to a good solution if Δt is too large). The norm of ψ_n is automatically preserved except if the method used to compute the exponential introduces errors violating the unitary.

A.3.3 Failure of the RK4 integrator for modelling the Optical Bloch Equations

Initially, the simulation of dynamics of the spin ensemble in the presence of thermal noises, was evolved using the RK4 numerical integrator. However, the final trajectory observed as shown in figure A.1a, was found to be different from literature and hence it was noticed that the RK4 was not a stable integrator for the integration of the Optical Bloch Equations.

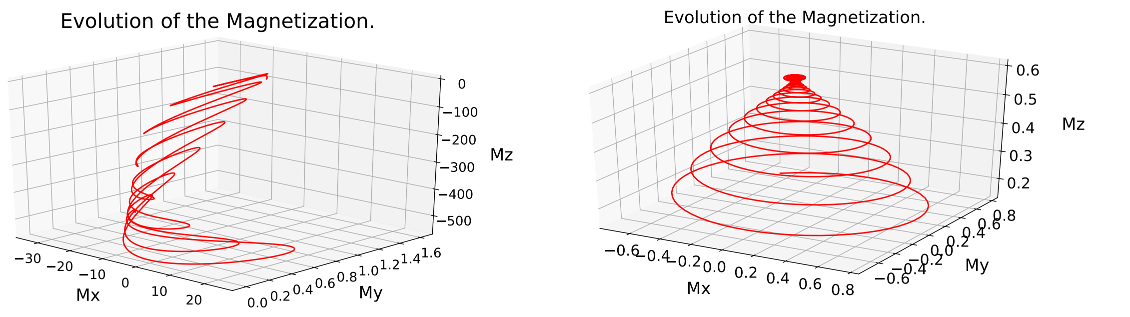

(A) Evolution of the magnetization vector using the RK4 integrator

(B) Evolution of the magnetization vector using the matrix exponential method

FIGURE A.1: Comparison of the integrators

We assume that the failure of this integrator is due to the discretization of steps and that the step size gets too small for the integrator to complete the computation or that the step size does not get small enough for the solution to track the "fast" dynamics of the system.

We are unable to find a good convergence for the system with the use of this integrator. The time scale of integration might be the reason that RK4 is a poor choice for the integration of OBE. To solve this problem, we make use of the matrix exponential integrator, to evolve the Bloch matrix through time. This is a higher dimension of the split operator method mentioned in section A.3.2. The temporal evolution of the magnetization vector using this integrator is given in figure A.1b

A.4 Reliability of the Program

The simulations produced using this program has been compared to literature. In case of the addition of the electromagnetic noises to the spin ensemble, we observe an extremely rapid fall in the coherence value, which is the expected result as mentioned in the article, "Importance of quantum decoherence in brain processes" by Max Tegmark [8]. Moreover, we have also tested this system for various values of the coupling constants and the results obtained are once again as mentioned in literature.

We have also tested the stability of the integrators used in this program. For the integration of the Schrödinger equation, we use the split operator method as it preserves the normalisation unlike in the case of another integrator such as the Richardson integrator. As mentioned in A.3.2, one of the major advantages of the split operator method is its unconditional stability implying good convergence even for a bad solution.

We also made an arbitrary choice of the famous Runge-Kutta fourth order integrator for the integration of the Dynamical systems and the Bloch Equations. On simulation, it was however realised that the RK4 integrator did not produce good results for the integration of the Optical Bloch Equations (OBE). This is analysed in the section A.3.3. Thus, this integrator was replaced by the matrix exponential method that produced the expected trajectories in phase space.

Bibliography

[1] Satoru Ishizuka and Hatsuo Hayashi. "Chaotic and phase-locked responses of the somatosensory cortex to a periodic medial lemniscus stimulation in the anesthetized rat". In: *Brain Research* 723.1 (1996), pp. 46–60. ISSN: 0006-8993. DOI: https://doi.org/10.1016/0006-8993(96)00214-4. URL: https://www.sciencedirect.com/science/article/pii/0006899396002144.

[2] David Viennot and Lucile Aubourg. "Decoherence, relaxation, and chaos in a kicked-spin ensemble". In: *Physical Review E* 87.6 (2013). ISSN: 1550-2376. DOI: 10.1103/physreve.87.062903. URL: http://dx.doi.org/10.1103/PhysRevE.87.062903.

[3] José Soto Alvarez. "Quantum-mechanical aspects of magnetic resonance imaging". In: *Revista Mexicana de Fisica* 63 (Jan. 2017), pp. 48–55.

[4] A.L. Hodgkin and A.F. Huxley. "A quantitative description of membrane current and its application to conduction and excitation in nerve". In: *Journal of Physiology* 117 (1952), pp. 500–544.

[5] Sundarapandian Vaidyanathan. "Adaptive Control of the FitzHugh-Nagumo Chaotic Neuron Model". In: *International Journal of PharmTech Research* 8 (Oct. 2015), pp. 117–127.

[6] Marko Marhl and Matjaž Perc. "Determining the flexibility of regular and chaotic attractors". In: *Chaos, Solitons & Fractals* 28 (May 2006), pp. 822–833. DOI: 10.1016/j.chaos.2005.08.013.

[7] Q. Ansel et al. "Optimizing fingerprinting experiments for parameter identification: Application to spin systems". In: *Phys. Rev. A* 96 (5 2017), p. 053419. DOI: 10.1103/PhysRevA.96.053419. URL: https://link.aps.org/doi/10.1103/PhysRevA.96.053419.

[8] Karlis Kanders, Tom Lorimer, and Ruedi Stoop. "Avalanche and edge-of-chaos criticality do not necessarily co-occur in neural networks". In: *Chaos: An Interdisciplinary Journal of Nonlinear Science* 27.4 (2017), p. 047408. DOI: 10.1063/1.4978998. eprint: https://doi.org/10.1063/1.4978998. URL: https://doi.org/10.1063/1.4978998.

[9] Petr Bob. "Chaos, brain and divided consciousness." In: *Acta Universitatis Carolinae. Medica. Monographia* 153 (Feb. 2007), pp. 9–80.

[10] Roger Penrose. *The Emperor's New Mind: Concerning Computers, Minds, and the Laws of Physics*. USA: Oxford University Press, Inc., 1989. ISBN: 0198519737.

[11] Max Tegmark. "Importance of quantum decoherence in brain processes". In: *Physical Review E* 61.4 (2000), 4194–4206. ISSN: 1095-3787. DOI: 10.1103/physreve.61.4194. URL: http://dx.doi.org/10.1103/PhysRevE.61.4194.

[12] Newton Howard et al. "BrainOS: A Novel Artificial Brain-Alike Automatic Machine Learning Framework". In: *Frontiers in Computational Neuroscience* 14 (2020), p. 16. ISSN: 1662-5188. DOI: 10.3389/fncom.2020.00016. URL: https://www.frontiersin.org/article/10.3389/fncom.2020.00016.